Research on Chemical Intermediates (2024) 50:2307–2324
https://doi.org/10.1007/s11164-024-05247-z

An efficient three-component one-pot synthesis of 3, 4-dihydropyrimidin-2-(1*H*)-thione derivatives with a mesoporous iron ion exchanged Indian clay catalyst

Mahesh Kancherla[1,3] · Kondaiah Seku[2] · Vijayakumar Badathala[3]

Received: 16 January 2024 / Accepted: 11 February 2024 / Published online: 13 March 2024

Abstract
This research work focuses on the potential usefulness of iron ion-exchanged Indian bentonite for one-pot synthesis of 3,4-dihydropyrimidine-2(1*H*)-thiones. Our goal was to produce mesoporous Fe^{3+}-exchanged Indian clay (Fe^{3+}-ExIC) and its supported forms through a wet impregnation technique. The physicochemical properties of the catalysts, such as XRD, FTIR, TGA, physisorption studies, SEM, and acidity, were investigated. It was found that Fe^{3+}-ExIC catalysts are efficient and reusable acidic heterogeneous catalysts for the synthesis of 3,4-dihydropyrimidine-2(1*H*)-thiones by refluxing aldehyde, methyl acetoacetate and thiourea with acetonitrile in cyclocondensation. An optimized reaction condition was found for preparing 5-methoxycarbonyl-6-methyl-4-phenyl-3,4-dihydropyrimidin-2(1*H*)-thione. A possible mechanism for the synthesis of 3,4-dihydropyrimidine-2(1*H*)-thiones has been proposed. Melting point, FTIR, and proton NMR were used to identify the products. Adequate catalyst activity was maintained over a period of six cycles, and a reduction in activity was attributed to a decrease in the acidity of the recycled catalyst.

Keywords Catalysis · Mesoporous clay catalyst · Fe^{3+}-ExIC · Biginelli reaction · Dihydropyrimidine-2(1*H*)-thione

✉ Kondaiah Seku
kondaiah.seku@utas.edu.om

✉ Vijayakumar Badathala
badathala@yahoo.com

1 Drug Standardization Research Unit, Regional Research Institute of Unani Medicine (NABH & NABL Accredited) (CCRUM, Ministry of AYUSH, Government of India, New Delhi), Chennai 600013, India

2 Engineering Department, College of Engineering and Technology, University of Technology and Applied Sciences, P.O. Box 77, 324 Shinas, Sultanate of Oman

3 Department of Chemistry, Vel Tech High Tech Dr. Rangarajan Dr.Sakunthala Engineering College (Autonomous), Avadi, Chennai 600 062, India

Introduction

In the pharmaceutical field, 3, 4-dihydropyrimidin-2(1*H*)-thiones (DHPT) are an important class of compounds capable of blocking calcium channel activity, inhibiting inflammation, and preventing cancer. In addition, DHPT is used as a biologically potent scaffold in adrenoreceptor antagonist activity, antihypertensive agents [1, 2], anticancer [3], antibacterial [4], antioxidant [5, 6], and antiviral compounds [7].

The use of multicomponent reactions enhances sustainable development since they allow for the synthesis of structurally diverse and complex organic molecules in one pot, in a clean, step-efficient manner, with high value-added, and thus contribute to the realization of a perfect synthesis [8, 9]and the associated environmental benefits [10–13]. Clays are readily available in nature. The clays are modified by various methods such as pillaring, supporting, intercalation and cation exchange. There are many advantages to using clay-supported reagents for organic synthesis[14–16], including their ease of availability, safety, reusability[17], enhanced selectivity [18], and cost-effectiveness. Various strategies are used to synthesize substituted 3, 4-dihydropyrimidin-2(1*H*)-thione motifs. The synthesis of these Biginelli organic molecules under green conditions is most advantageous using the one-pot three-component condensation reaction. A lot of effort has been put into developing an easy and simple protocol for the synthesis of substituted 3, 4-dihydropyridine-2 (1*H*)-thiones by using catalysts including sulfated tungstate [19], Hydrotalcite [20], $ZrOCl_2$/mont K10 [21], CSC-Star-SO_3-$AlCl_2$ [22], $H_5PW_{10}V_2O_{40}$/Pip-SBA-15 [23], Nano ZnO [24], Cellulose sulfuric acid [25], MnO_2–MWCNT [26], SiO_2–$CuCl_2$ [27], Mo/γ-Al_2O_3 [28], Nanosized TiO_2–SiO_2 [29], Bi(III) complex of Fe_3O_4/SiO_2-NH-ligand [30], Polyethylene-supported Fe/ionic liquid complex [31], Fe_3O_4@SiO_2-APTMS-$Fe(OH)_2$ [32], dendrimer-attached phosphotungstic acid nanoparticles immobilized on nanosilica [33], Polyionene/Br_3 grafted on magnetic nanoparticles [34], strontium pyroarsenate nano-plates [35], N-Methylimidazolium acetate [36], and TiO_2 nanoparticles [37], Acridine Yellow G [38, 39]. Fe^{+3}-montmorillonite K-10 [40] catalyst had been reported for the synthesis of Biginelli compounds. Montmorillonite K-10 is an acid-treated catalyst that was further treated with $FeCl_3$, which was not characterized by the researchers. In spite of these catalysts being effective for the synthesis of Biginelli derivatives, they are limited by molar ratios, catalyst amounts, reaction times, and homogeneity of the reaction medium.

Several substituted 3, 4-dihydropyrimidin-2(1*H*)-thiones have been synthesized using Fe^{3+}-ExIC as a catalyst to overcome such drawbacks. Catalytic systems were developed using different strategies in the present study. The resulting catalysts were characterized by XRD, FTIR, TGA, BET surface area, BJH pore distribution, and SEM. Further, to find their acidity, the DRIFTS method was employed. In addition, the reduced activity of the catalysts after reuse has been studied by measuring the acidity of the reused clay catalyst for the first time.

Materials and methods

The Indian clay samples used in this study were purchased from Ashapura Group of Industries, India. Deionized water was used in the modification of the clay catalysts. The reactants were procured from Avra synthesis and Fischer-Scientific. *p*-Toluene sulphonic acid monohydrate (98%, *p*-TSA.H_2O), 12-tungstophosphoric acid (98%, PWA), and zirconiumoxychloride octahydrate (98%, $ZrOCl_2.8H_2O$) were received from Loba Chemie Pvt. Ltd., India. Some solvents were utilized as such and others were distilled for purification.

Preparation of the catalysts

Iron ion exchanged Indian clay (Fe^{3+}-ExIC)

5 g of Indian clay is added to 200 ml of 0.5 M aqueous $FeCl_3$ solution. A continuous exchange procedure took place at room temperature for 16 h. The slurry was centrifuged repeatedly using fresh deionized water until it was free of chloride ions [by silver nitrate test]. After being dried overnight at 100 °C, the solid was ground into a fine powder.

p-TSA supported on Fe^{3+}-ExIC

A homogeneous solution was formed by dissolving 750 mg (15 wt %) of *p*-toluene sulphonic acid monohydrate in 50 ml of methanol. Continuous stirring was used to mix methanolic *p*-TSA.H_2O with 5 g of Fe^{3+}-ExIC. A vacuum pump was used to remove the solvent from the methanolic *p*-TSA.H_2O with Fe^{3+}-ExIC and then the powder was dried in an oven for 3 h at 100 °C to obtain *p*-TSA/Fe^{3+}-ExIC.

PWA supported on Fe^{3+}-ExIC

In 50 ml of methanol, 750 mg (15 wt %) of 12-tungstophosphoric acid (PWA) was dissolved to form a homogeneous solution. With constant stirring, 5 g of Fe^{3+}-ExIC was slowly added to the methanolic PWA solution. PWA/Fe^{3+}-ExIC was obtained using a vacuum by removing the solvent and drying it at 100 °C for three hours.

$ZrOCl_2$ supported on Fe^{3+}-ExIC

The zirconium oxychloride octahydrate ($ZrOCl_2.8H_2O$) solution was prepared by dissolving 750 mg (15 wt %) in 50 ml of methanol. In a constant stirring process,

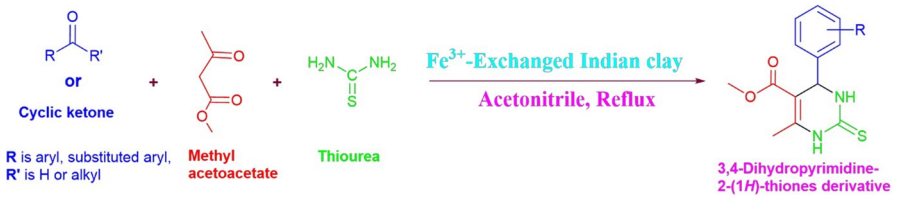

Scheme 1 Synthesis of 3, 4-dihydropyrimidin-2(1*H*)-thione derivatives

5 g of Fe^{3+}-ExIC was slowly added to a solution of methanolic $ZrOCl_2$. Under vacuum, the solvent was removed from the powder, which was then dried at 100 °C for three hours to yield $ZrOCl_2/Fe^{3+}$-ExIC.

Characterization of the catalysts

An X-ray diffractometer with a Rigaku XPert Pro was used to analyze clay catalysts. PXRD measurements were performed between 4° and 70°. With a JASCO 4600 FTIR spectrometer in transmittance mode, IR spectra were recorded between 400 and 4000 cm^{-1} using 32 scans for clay catalysts and organic products (KBr pellet method). On the TA SDT Q600 model instrument, thermo gravimetric analysis of clay catalysts (TGA) was done in nitrogen atmosphere (50 ml/min) with linear heating from room temperature to 800 °C. The specific surface areas of clay samples were determined by N_2 adsorption–desorption at 77 K using a Micromeritics ASAP 2020 surface area analyzer, and the pore diameters were determined by Barrett-Joyner-Halenda (BJH) by studying the desorption branch of the isotherm. In a dynamic vacuum, samples were degassed at 150 °C for 12 h before sorbometric analysis was conducted. SEM morphology analysis was performed using a microscope LEO 1450. Several Biginelli products were tested using open capillaries. Bruker 300 MHz NMR spectrometer was used to record the ^1H NMR spectra of organic compounds. Pyridine was used as a probe molecule for determining the acidity of fresh and recycled Fe^{3+}-ExIC catalysts using diffuse reflection Infrared Fourier Transform spectroscopy (DRIFTS) [41].

Catalytic activity study

Fe^{3+}-ExIC and its modified forms were evaluated for their catalytic activity for the synthesis of 3, 4-dihydropyrimidin-2(1*H*)-thiones (Scheme 1). For the production of 3, 4-dihydropyrimidin-2(1*H*)-thiones, acetonitrile medium, aldehyde or ketone (1 mmol), thiourea (3 mmol), and methyl acetoacetate (1 mmol) were refluxed together with catalyst. An analysis of the reaction progress was conducted using thin-layer chromatography. Catalytic activity was also assessed using a variety of catalysts, solvents, catalyst amounts, molar ratios of reactants, and time intervals. The catalyst was isolated after cooling and filtering the reaction mixture to room temperature. Following the evaporation of the solvent, the crude product was poured onto crushed ice and thoroughly mixed for five minutes. A 3, 4-dihydropyrimidin-2(1*H*)-thione

product was obtained following filtration and additional purification with ethanol. The products were identified by melting points, IR specta, and NMR spectra.

Results and discussion

Characterization of Fe^{3+}-ExIC& its modified forms

Figure 1 shows the PXRD patterns of Fe^{3+}-ExIC together with its modified forms. As shown in Fig. 1, the peak at 6.82° corresponds to the periodicity in the direction of (0 01) for Fe^{3+}-ExIC samples with a basal spacing of 12.96 Å. Observed peaks of the Fe^{3+}-ExIC catalyst are 6.82°, 20.28°, 27.19°, 28.65°, and 35.92°. Supported catalysts are not altering their basal spacing values. Compared to the parent material, Fe^{3+}-ExICs on support showed only a small increase in the XRD peak intensity. It may be due to *p*-TSA, PWA, and $ZrOCl_2$ adsorption on Fe^{3+}-ExIC.

An FTIR spectrum of Fe^{3+}-ExIC and its supported catalysts is shown in Fig. 2. A band at 3634 cm^{-1} corresponds to hydroxyls in the lattice. Stretching in the interlayer or bending in the surface water is responsible for the Infrared bands at 3426 and 1643 cm^{-1}. A strong shoulder band has been observed at 1119 cm^{-1} associated with the Si–O bending vibrations, while another strong band has been observed at 1029 cm^{-1} associated with the Si–O–Si stretching vibrations. There was a shoulder band corresponding to the Al–O–H group at 916 cm^{-1} and a shoulder band at 878 cm^{-1} due to the skeletal vibrations of quartz. In *p*-TSA/Fe^{3+}-ExIC, an extra peak at 690 cm^{-1} may be attributed to the influence of *p*-TSA [37], and in PWA/Fe^{3+}-ExIC a band at 802 cm^{-1} may be assigned to the vibration of W–O–W. Despite this, in *p*-TSA/Fe^{3+}-ExIC, PWA/Fe^{3+}-ExIC and $ZrOCl_2$/Fe^{3+}-ExIC, all other bands corresponding to the parent clay, Fe^{3+}-ExIC, were not visible and merged with those of *p*-TSA, PWA, and $ZrOCl_2$.

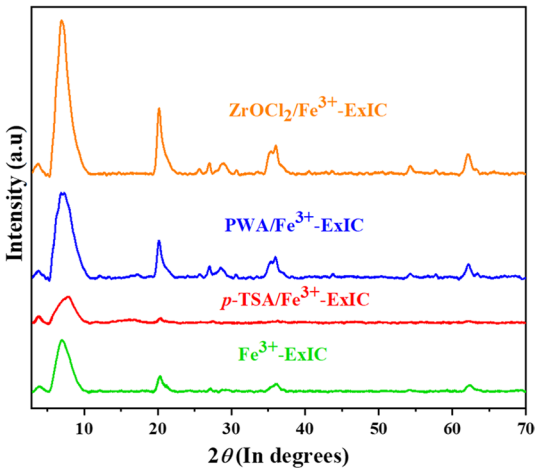

Fig. 1 XRD ofFe^{3+}-ExIC, *p*-TSA/Fe^{3+}-ExIC, PWA/Fe^{3+}-ExIC and $ZrOCl_2$/Fe^{3+}-ExIC

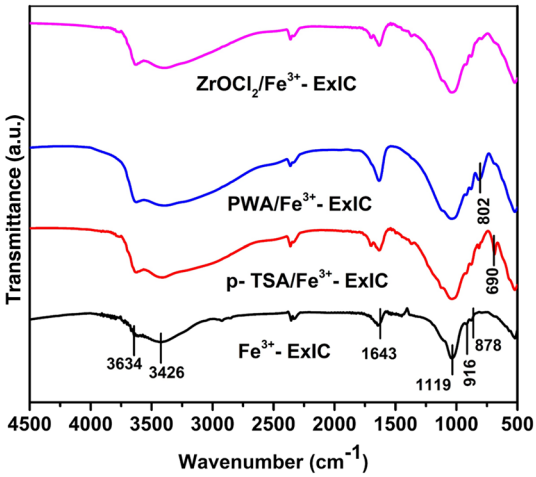

Fig. 2 FT-IR spectra of Fe^{3+}-ExIC, *p*-TSA/Fe^{3+}-ExIC, PWA/Fe^{3+}-ExIC and $ZrOCl_2$/Fe^{3+}-ExIC

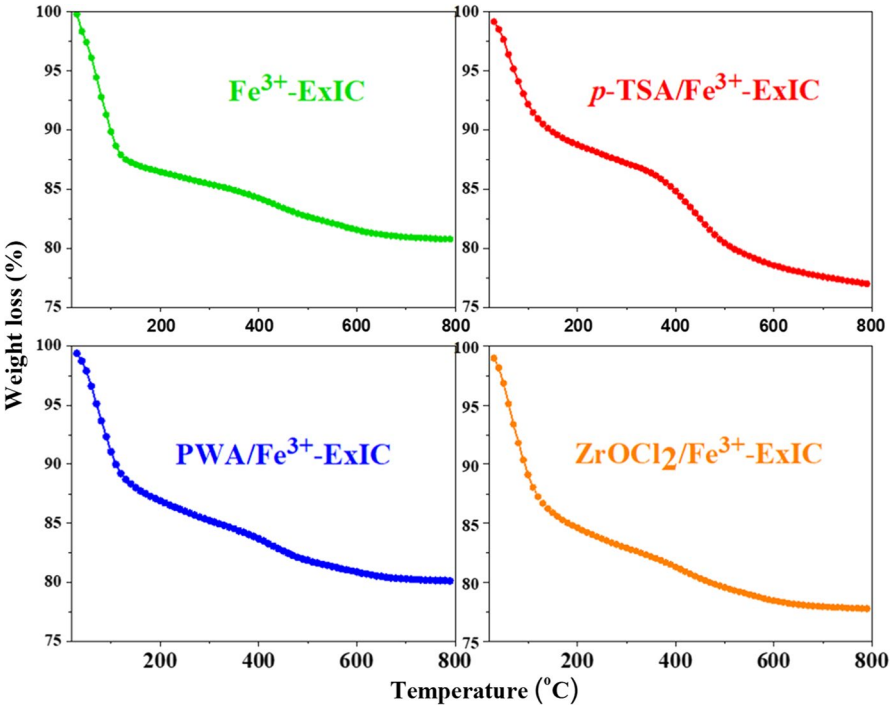

Fig. 3 Thermogravimetric profiles of Fe^{3+}-ExIC, *p*-TSA/Fe^{3+}-ExIC, PWA/Fe^{3+}-ExIC and $ZrOCl_2$/Fe^{3+}-ExIC

Figure 3 shows the TGA profiles of air-dried Fe^{3+}-ExIC, *p*-TSA/Fe^{3+}-ExIC, PWA/Fe^{3+}-ExIC, and $ZrOCl_2$ /Fe^{3+}-ExIC catalysts. The PWA/Fe^{3+}-ExIC and Fe^{3+}-ExIC catalysts show a sharp drop in weight at about 150 °C due to the loss of

water physically adsorbed to them and a second drop beyond that due to the loss of hydroxyl groups [42, 43]. Gradual weight loss detectable at 400–700 °C indicates that clay's structure is associated with hydroxyl water, which also indicates the thermal stability of PWA on Fe^{3+}-ExIC. It is evident from the TGA profile of *p*-TSA/Fe^{3+}-ExIC that the initial sharp decrease in weight is caused by the loss of physically adsorbed water and interlayer water, followed by a gradual reduction in weight after 120–350 °C due to hydroxyl group losses and dehydration. In the range of 350–800 °C, hydroxyl water is lost because of the structure of *p*-TSA and its gradual decomposition. However, when the TGA curve of Fe^{3+}-ExIC/$ZrOCl_2$ is investigated within the temperature range of 80–150 °C, Fe^{3+}-ExIC and $ZrOCl_2.8H_2O$ exhibit an initial sharp decrease in weight due to loss of adsorbed water and hydration water, and the removal of HCl. The gradual dehydration of $ZrOCl_2.8H_2O$ and hydroxyl water associated with clay's structure causes it to lose 8% weight as it is heated from 150 to 700 °C. Therefore, $ZrOCl_2$ binds heterogeneously to Fe^{3+}-ExIC. The possible explanations concluded that the formation of intermolecular bonds between Fe^{3+}-ExIC and $ZrOCl_2$.

The surface areas of the supported Fe^{3+}-ExIC catalysts and pore sizes(adsorption branch) have been calculated. The isotherms of adsorption–desorption of nitrogen

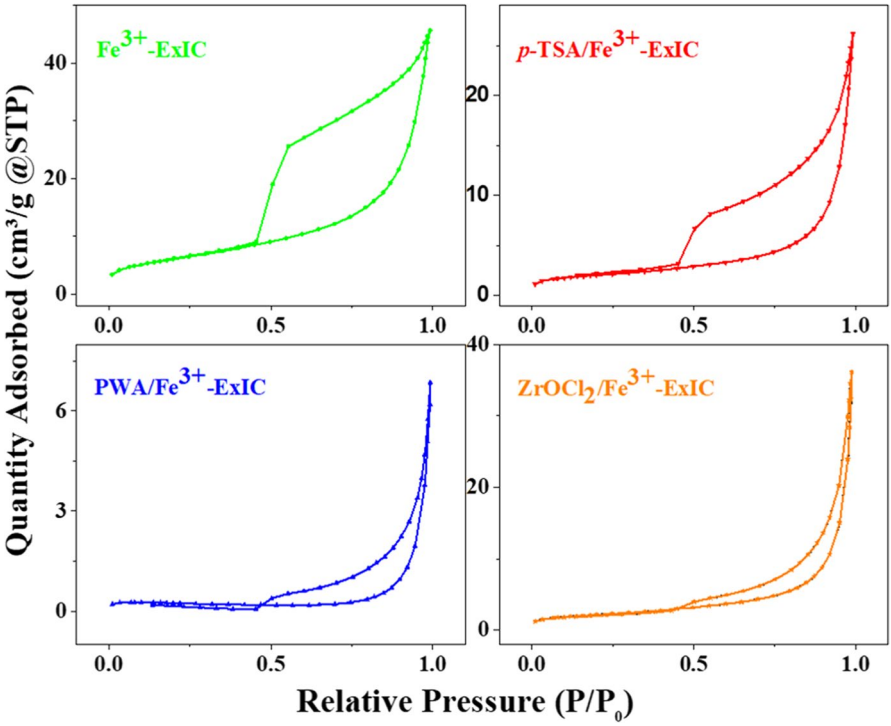

Fig. 4 Nitrogen adsorption–desorption isotherms of Fe^{3+}-ExIC,*p*-TSA/Fe^{3+}-ExIC, PWA/Fe^{3+}-ExIC and $ZrOCl_2$/Fe^{3+}-ExIC

for Fe^{3+}-ExIC, *p*-TSA/Fe^{3+}-ExIC, PWA/Fe^{3+}-ExIC, and $ZrOCl_2$/Fe^{3+}-ExIC are shown in Fig. 4. Hysteresis loops are observed for catalysts in the 0.45 to 0.99 relative pressure range. However, Fe^{3+}-ExIC and *p*-TSA/Fe^{3+}-ExIC exhibit slightly bigger hysteresis loops compared to PWA/Fe^{3+}-ExIC, and $ZrOCl_2$ /Fe^{3+}-ExIC in the relative pressure (P/Po) range of 0.45–0.99. Catalyst sorption isotherms (H3) indicate slit-shaped and panel-shaped pores [42]. In Fig. 5, there are curves for *p*-TSA/Fe^{3+}-ExIC, PWA/Fe^{3+}-ExIC, and $ZrOCl_2$/Fe^{3+}-ExIC distributions of pore size according to BJH. Modified forms possess mesopores and macropores, whereas PWA/Fe^{3+}-ExIC has macropores. The average pore diameters of the modified forms have increased, and $ZrOCl_2$/Fe^{3+}-ExIC contains mesopores and macropores. Due to the adsorption process, the supported catalysts have a lower specific surface area (Table 1) than the patent clay.

Figure 6 illustrates the surface morphology of Fe^{3+}-ExIC, *p*-TSA/Fe^{3+}-ExIC, PWA/Fe^{3+}-ExIC, and $ZrOCl_2$/Fe^{3+}-ExIC. The SEM images of samples containing the microsphere size ranging from 30 to 150 nm were observed. In the SEM image of Fe^{3+}-ExIC, irregular stoned shapes with different sizes were observed, with an average particle size of 35 nm. Particles were free of agglomeration. In the SEM images of *p*-TSA/Fe^{3+}-ExIC, PWA/Fe^{3+}-ExIC and $ZrOCl_2$/Fe^{3+}-ExIC showed irregular agglomerated stoned-shaped particles with different sizes having an average size of 60 nm, 75 and 120 nm respectively. It was found that these results were

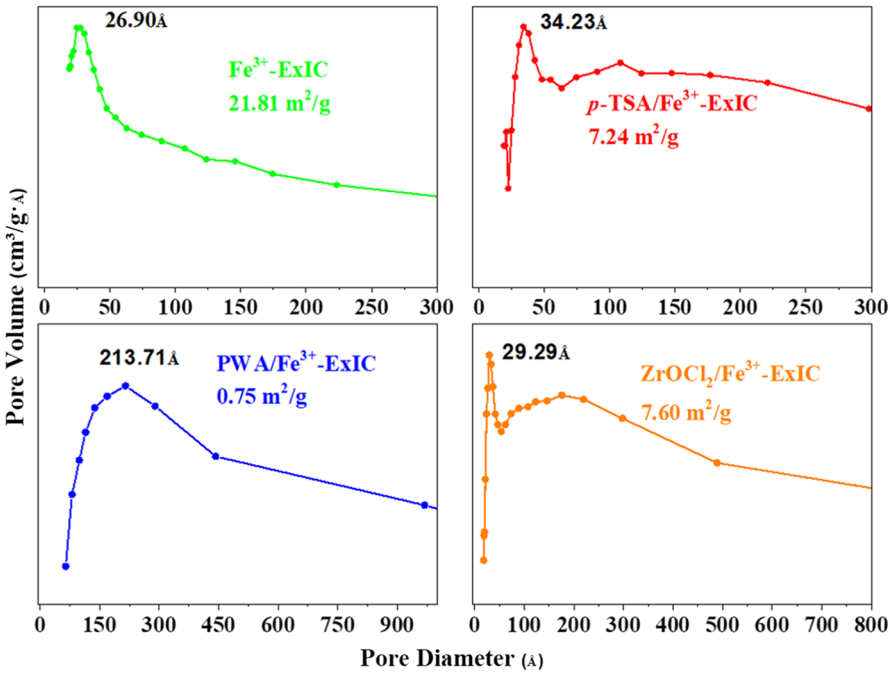

Fig. 5 BJH pore size distribution curves of Fe^{3+}-ExIC, *p*-TSA/Fe^{3+}-ExIC, PWA/Fe^{3+}-ExIC and $ZrOCl_2$/Fe^{3+}-ExIC

Table 1 Activity of catalysts for synthesis of 5-methoxycarbonyl-6-methyl-4-phenyl-3, 4-dihydropyrimidin-2(1*H*)-thione

Entry	Catalyst	BET surface area (m^2/g)	Time (h)	Yield (%)*
1	Montmorillonite K10	155	4	50
2	Montmorillonite K30	138	4	30
3	Al^{3+}-ExIC	76	4	16
4	Fe^{3+}-ExIC	21	4	23
5	*p*-TSA/mont K10	40	4	40
6	*p*-TSA/mont K30 Montmorillonite-K30	59	4	34
7	PWA/mont K10	–	4	25
8	PWA/mont K30	111	4	38
9	PWA/Al^{3+}-ExIC	1.81	4	43
10	*p*-TSA/Al^{3+}-ExIC	3.14	4	20
11	$ZrOCl_2$/Al^{3+}-ExIC	8.07	4	15
12	*p*-TSA/Fe^{3+}-ExIC	7.24	4	26
13	PWA/ Fe^{3+}-ExIC	0.75	4	44
14	$ZrOCl_2$/Fe^{3+}-ExIC	7.60	4	29
15	H_3BO_3/mont K10	89	4	47
16	H_3BO_3/mont K30	78	4	42

*Isolated yields. Reaction conditions: Molar ratio of Benzaldehyde: Methylacetoacetate: Thiourea = 1:1:1 (3 mmol), Catalyst: 150 mg, Ethanol: 10 ml, Time: 4 h

in agreement with the BET surface area. Therefore, the modified catalysts have a higher level of particle aggregation than their parent clay.

After pyridine adsorption, the DRIFTS spectra of Fe^{3+}-ExIC, *p*-TSA/Fe^{3+}-ExIC, PWA/Fe^{3+}-ExIC, and $ZrOCl_2$/Fe^{3+}-ExIC are shown in Fig. 7.

This technique can qualitatively determine an acidic site on the catalyst surface. After modification, the catalysts showed improved acidity [44]. It has been demonstrated that modified catalysts have a higher density of Brønsted acid sites at 1545 cm^{-1} and Lewis's acid sites at 1490 cm^{-1}, compared to Fe^{3+}-ExIC. A small decrease in Lewis's acidity can be observed in *p*-TSA/Fe^{3+}-ExIC, PWA/Fe3 + -ExIC, and $ZrOCl_2$/Fe^{3+}-ExIC at 1442 cm^{-1}.

Catalytic studies for the synthesis of 3, 4-dihydropyrimidin-2(1*H*)-thiones

Clay catalysts (150 mg, Table 1) are tested for their catalytic activity to determine which one is best suited for synthesizing 5-methoxycarbonyl-6-methyl-4-phenyl-3, 4-dihydropyrimidin-2(1*H*)-thione by using ethanol solvent to react equimolar quantities of aryl aldehydes, thiourea and methyl acetoacetate in one pot. The catalysts have shown improved activity after modification. However, the results didn't give a conclusion on the selection of a catalyst for the reaction under study.

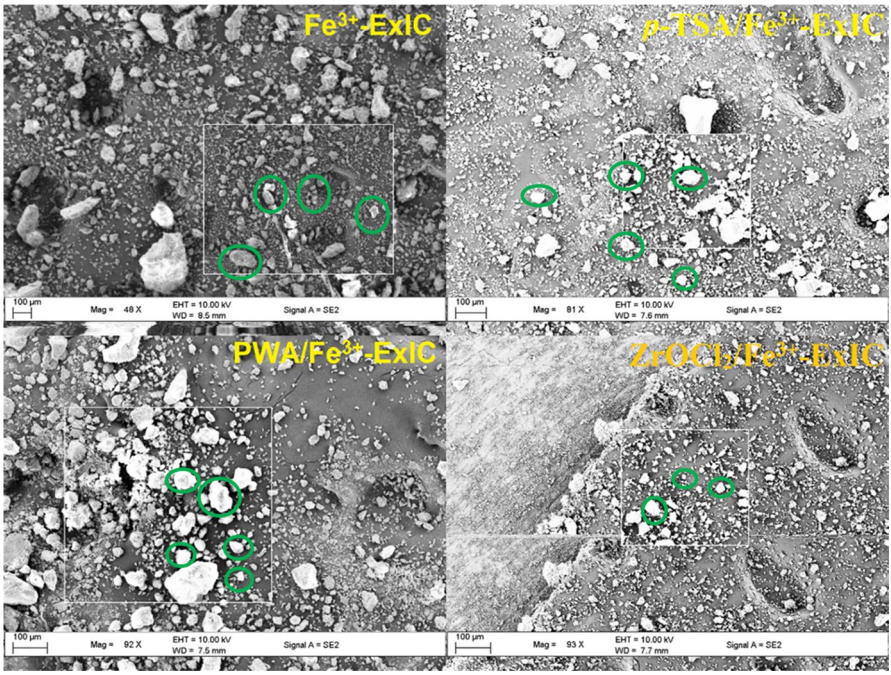

Fig. 6 SEM images of Fe^{3+}-ExIC, *p*-TSA/Fe^{3+}-ExIC, PWA/Fe^{3+}-ExIC and $ZrOCl_2$/Fe^{3+}-ExIC

In methanol, ethanol, and acetonitrile solvents, a few iron-based clay catalysts were tested as catalysts for 5-methoxycarbonyl-6-methyl-4-phenyl-3, 4-dihydropyrimidin-2(1*H*)-thione synthesis (Table 2). Table 2 depicts the activity under specified conditions:

In acetonitrile solvent: Fe^{3+}-ExIC > $ZrOCl_2$/Fe^{3+}-ExIC > $FeCl_3$/mont K10 > *p*-TSA/ Fe^{3+}-ExIC > PWA/Fe^{3+}-ExIC.

In ethanol solvent: $ZrOCl_2$/Fe^{3+}-ExIC > $FeCl_3$/mont K10 > Fe^{3+}-ExIC > *p*-TSA/ Fe^{3+}-ExIC > PWA/Fe^{3+}-ExIC.

In methanol solvent: $FeCl_3$/mont K10 > PWA/Fe^{3+}-ExIC > $ZrOCl_2$/Fe^{3+}-ExIC > Fe^{3+}-ExIC > *p*-TSA/ Fe^{3+}-ExIC.

Table 2 shows that Fe^{3+}-ExIC can be used as a catalyst for benzaldehyde, methyl acetoacetate, and excess thiourea reactions and that the yield of 5-methoxycarbonyl-6-methyl-4-phenyl-3,4-dihydropyridin-2 (1*H*)-thione was affected by a variety of parameters including solvent, molar ratio, catalyst amount, and time. Furthermore, various 3,4-dihydropyrimidin-2(1*H*)-thiones were synthesized under optimal conditions, and Fe^{3+}-ExIC's recyclability was examined.

Seven solvents were used to investigate the effect of the reaction medium (Fig. 8a). 5-methoxycarbonyl-6-methyl-4-phenyl-3,4-dihydropyrimidin-2(1*H*)-thione was prepared in acetonitrile with a maximum yield of 97%. However, there was no reaction in the water. It was also observed that the yields were 59% and 63% in toluene and *o*-xylene (non-polar solvents), respectively. The yields were 67%, 81%, and 54% in methanol, ethanol, and *n*-butanol, respectively. Therefore,

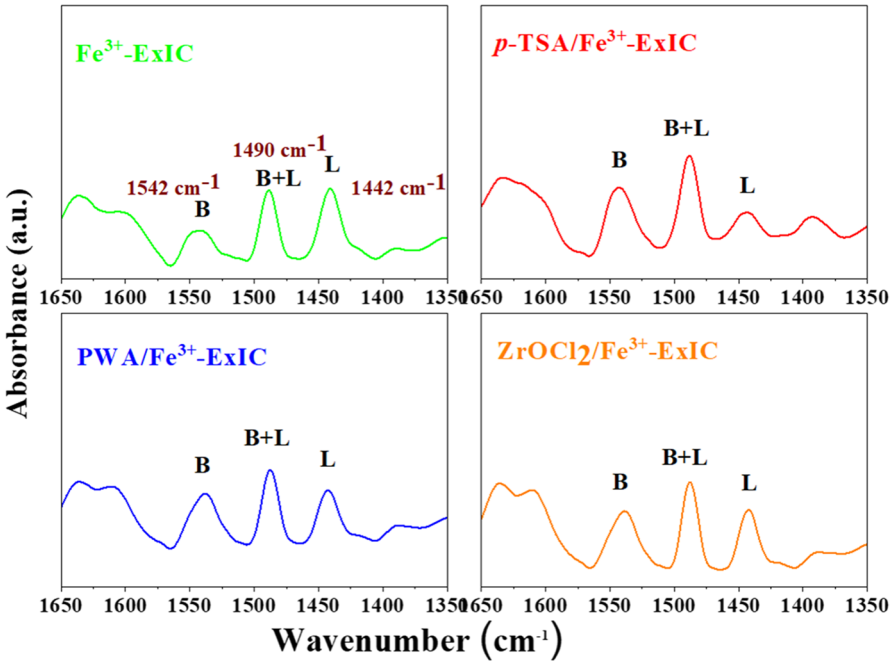

Fig. 7 DRIFTS spectra of Fe^{3+}-ExIC, *p*-TSA/Fe^{3+}-ExIC, PWA/Fe^{3+}-ExIC and $ZrOCl_2$/Fe^{3+}-ExIC after pyridine adsorption

Table 2 Activity of few supported catalysts for the synthesis of 5-methoxycarbonyl-6-methyl-4-phenyl-3,4-dihydropyrimidin-2(1*H*)-thione

Entry	Catalyst	Yield (%)* in methanol	Yield (%)* in ethanol	Yield (%)* in acetonitrile
1	$FeCl_3$/mont K10	73	83	85
2	$ZrOCl_2$/Fe^{3+}-ExIC	69	85	89
3	*p*-TSA/Fe^{3+}-ExIC	40	77	69
4	Fe^{3+}-ExIC	67	81	97
5	PWA/Fe^{3+}-ExIC	72	57	53

*Isolated yields. Reaction conditions: Molar ratio of Benzaldehyde: Methyl acetoacetate: Thiourea = 1:1:3, Catalyst: 150 mg, Solvent: 10 ml, Time: 4 h

further reactions were studied in acetonitrile solvent. Thus, the reaction conditions, such as catalyst selection and solvent selection, were optimized [45].

The effect of the amount of catalyst has been investigated under optimized reaction conditions using 50–300 mg of Fe^{3+}-ExIC catalyst for 4 h. With increasing catalyst amounts, 5-methoxycarbonyl-6-methyl-4-phenyl-3,4-dihydropyrimidin-2(1*H*)-thione yields increased (Fig. 8b). The product yield gradually decreased after using 200–300 mg of catalyst. Consequently, the lower yield of

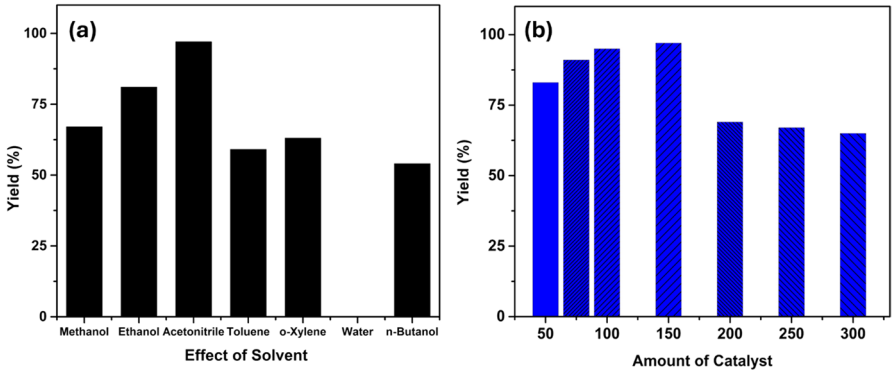

Fig. 8 **a** Effect of solvent and **b** Effect of amount of the catalyst

the product with excess catalyst can be attributed to the restricted diffusion of the desired product within the active sites as a result of the increased adsorption of the desired product on the superfluous active sites, which was likely caused by an inappropriate solvation medium [36]. The preparation of 5-methyl-6-phenyl-4-phenyl-3,4-dihydropyrimidin-2(1*H*)-thione was inhibited when catalyst quantities were increased. It was determined that 50 mg of catalyst should be used to synthesize 3,4-dihydropyrimidin-2(1*H*)-thiones.

The reaction of benzaldehyde, methyl acetoacetate, and thiourea with Fe^{3+}-ExIC was carried out at various molar ratios (Fig. 9a). By increasing the molar ratio of benzaldehyde to methyl acetoacetate and thiourea from 1:0.5 to 1:3.5, a greater quantity of the product was formed. When the concentration of thiourea is increased, the equilibrium shifts toward the formation of 5-methoxycarbonyl-6-methyl-4-phenyl-3,4-dihydropyrimidin-2(1*H*)-thione. There was no effect on the percentage yield of 5-methoxycarbonyl-6-methyl-4-phenyl-3,4-dihydropyrimidin-2(1*H*)-thione (97) when the benzaldehyde/methyl acetoacetate/thiourea ratio was over 3:1. It was determined that a molar ratio of

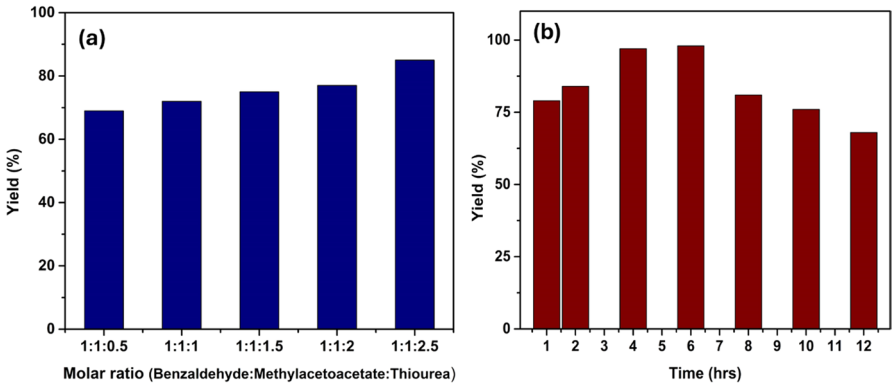

Fig. 9 **a** Effect of molar ratio and **b** Effect of time

1:1:3 (benzaldehyde: methyl acetoacetate: thiourea) would facilitate further investigation.

At seven intervals of time, Fe^{3+}-ExIC catalyzed the reaction of benzaldehyde, methyl acetoacetate, and thiourea in acetonitrile. A decrease in yield occurs with increasing reaction time from 1 to 6 h, followed by an increase in yield with increasing reaction time (Fig. 9b). The decomposition of unreacted reactants and the formation of products due to prolonged heating can cause this phenomenon. The optimized reaction conditions were evaluated by using different aldehydes/ketones, thiourea, and the -keto ester in acetonitrile under reflux for 4 h.

The results of synthesized derivatives of 3,4-dihydropyrimidin-2(1*H*)-thione are given in Table 3. There were 75–80% yields of dihydropyrimidin-2(1*H*)-thiones produced by 3-nitro, 4-nitro, and 3,4-dimethoxy substituted benzaldehydes, and 62–72% yields of dihydropyrimidin-2(1*H*)-thiones produced by 2-nitro, 4-chloro, and 2-hydroxyl substituted benzaldehydes, compared to 66% and 58% yields for cinnamonaldehyde and 2-chlorobenzaldehyde, respectively. The yields of dihydropyrimidin-2(1*H*)-thione from acetophenone and halo-substituted acetophenone were 55–62%. A 51% yield was obtained with cyclopentanone, while a 54% yield was obtained with cyclohexanone (Table 3). The reactions produce lower yields due to a retarding effect.

In Scheme 2, the reaction proceeds via the acylimine intermediate (3) formed by the reaction of aldehyde (1) and thiourea (2), catalyzed by Fe^{3+}-ExIC. An enolate keto ester (4) was added to the acylimine, followed by cyclization and the elimination of water to obtain 3, 4-dihydropyrimidin-2(1*H*)-thione (5).

Recyclability of Fe^{3+}-ExIC

For the preparation of 5-methoxycarbonyl-6-methyl-4-phenyl-3,4-dihydropyrimidin-2(1*H*)-thione, benzaldehyde (1 mmol) and methyl acetoacetate (1 mmol) were refluxed in acetonitrile medium for 4 h with the regenerated catalyst (150 mg). As shown in Fig. 10, the Fe^{3+}-ExIC gradually lost its activity when regenerated. The reused catalyst had the same activity in both the first and second cycles. The yield declined by 3% in the third cycle, and another 3% in the fourth cycle. Despite the fact that the activity of the recycled catalyst was gradually decreasing, the percentage yield in all of these reactions was greater than 90%. However, the fifth, sixth, and seventh cycles had yield losses of 11%, 13%, and 16%, respectively. The reused catalyst's gradual loss of activity is owing to its decreased acidity, as detailed in the following section.

DRIFTS of reused Fe^{3+}-ExIC

Catalysts were separated after completion of the reaction by filtration, washed with dichloromethane, and activated at 110 °C. Using pyridine as a probe molecule, DRIFTS technique was used to determine the acidity of the reused catalyst. Generally, organic reactions can be catalyzed by a clay catalyst that functions as a Brønsted acid, Lewis's acid, or both [16]. Figure 11 depicts a comparative study of fresh

Table 3 Fe^{3+}-ExIC catalyzed synthesis of 3,4-dihydropyrimidin-2(1*H*)-thione derivatives

Entry	Aldehyde/ Ketone	Methyl acetoacetate	Thiourea	Product	Yield (%)*	Melting Point (°C)
1		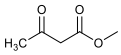		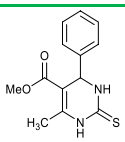	97	158-160
2		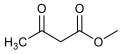		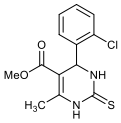	58	178-180
3	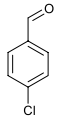	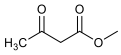		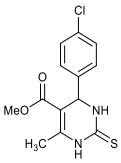	64	152-154
4		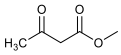		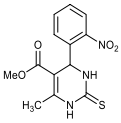	62	159-161
5		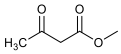		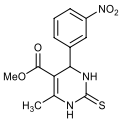	80	162-164
6	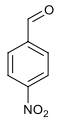	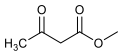		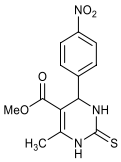	75	160-162
7		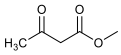		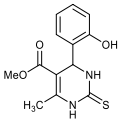	72	140-142
8	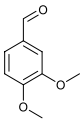	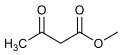		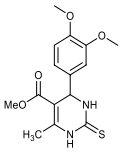	79	126-128

*Isolated yield. Reaction conditions: Molar ratio (Benzaldehyde: Methylacetoacetate: Thiourea) = 1:1:3, Amount of catalyst: 150 mg, Solvent: Acetonitrile, Time: 4 h

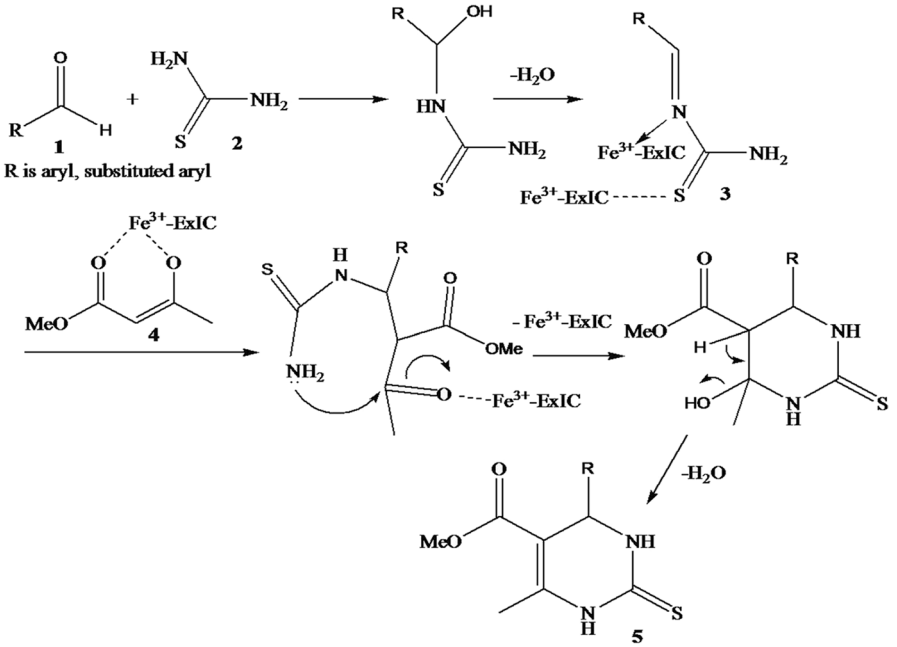

Scheme 2 Conjecture mechanism for the synthesis of 3,4-dihydropyrimidin-2(1*H*)-thiones catalyzed by Fe^{3+}-ExIC

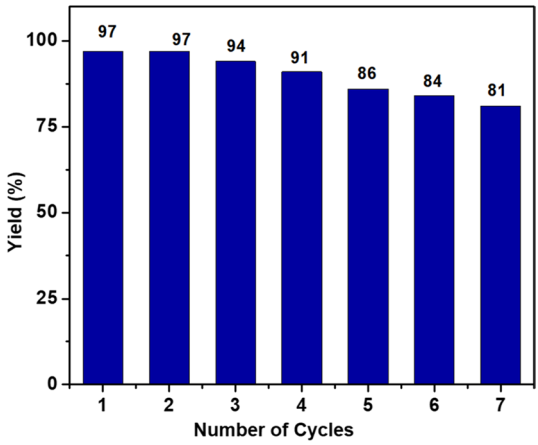

Fig. 10 Reusability of Fe^{3+}-ExIC

& reused Fe^{3+}-ExIC catalyst with respect to the acidic sites on its surface which are responsible for organic transformations. The reused catalyst has shown reduced acidity after reuse. The densities of Brønsted acid sites at 1545 cm^{-1}, Brønsted and Lewis acid sites at 1490 $cm^{-1}$and Lewis acidic sites at 1442 cm^{-1} were reduced. This can be attributed to the gradual loss in the catalytic activity of Fe^{3+}-ExIC after reuse.

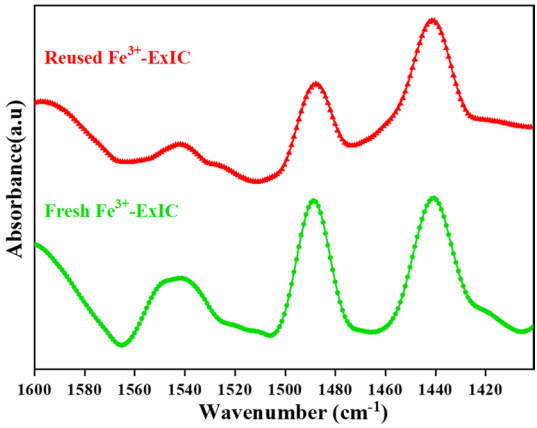

Fig. 11 DRIFTS spectra of fresh and reused Fe^{3+}-ExIC

Conclusions

A one-pot synthesis of 3,4-dihydropyrimidin-2 (1*H*)-thiones using a mesoporous Fe^{3+}–ExIC heterogeneous clay catalyst is described in this study. It is simple, inexpensive, reusable, and eco-friendly. Three supported catalysts of Fe^{3+}-ExIC have been prepared and characterized. In order to confirm the acidic nature of the catalysts, the DRIFTS method was applied after pyridine adsorption. 5-methoxycarbonyl-6-methyl-4-phenyl-3,4-dihydropyrimidin-2(1*H*)-thione was synthesized by Fe^{3+}-ExIC. Under optimized conditions, various substituted 3, 4-dihydropyrimidin-2(1*H*)-thiones have been synthesized in good to excellent yields. Until six cycles, the catalyst under green standards will retain its activity without a substantial loss. By investigating the reduced acidic nature (Brønsted & Lewis) of the reused catalyst, the catalyst's gradual loss of catalytic activity was further explained. The iron ion exchanged Indian clay catalyst can be recommended to prepare several useful organic compounds such as coumarins, 2,3-dihydroquinazolin-4(1*H*)-ones, esters, imidazoles, etc. As a result of its unique properties, such as its large surface area and high catalytic activity, it is also useful as a catalyst in a wide variety of chemical reactions as well as pharmaceutical intermediates.

Acknowledgements BVK is thankful to the SERB, Ministry of DST, Government of India for sanctioning the research project (Project No. SB/FT/CS-089/2012). The authors thank Vel Tech High Tech Dr. RR Dr.SR Engineering College for providing research facilities.

Authors contributions MK: Experimental and Characterization work analysis; KS: Data analysis, Visualization, and Characterization work analysis; VB: Conceptualization, Investigation, Writing-Original Draft, Funding Acquisition.

Funding The SERB, Ministry of DST, Government of India had provided financial support for this study (Project No. SB/FT/CS-089/2012).

Data availability Data will be made available upon reasonable request.

Declarations

Conflict of interest The authors have no competing interests to declare that are relevant to the content of this article.

Ethical approval and consent to participate Does not require any ethical approval since we could not use any animals or Humans for this study.

References

1. K.S. Atwal, B.N. Swanson, S.E. Unger, D.M. Floyd, S. Moreland, A. Hedberg, B.C. O'Reilly, J. Med. Chem. **34**, 806 (1991)
2. C.O. Kappe, Eur. J. Med. Chem. **35**, 1043 (2000)
3. W.M.B.I.A. Nagwa, M. Abdelazeem Farid, M. Sroor, M.A. Tantawy, Polycycl. Aromat. Compd. **43**, 5840 (2023)
4. M. Brands, R. Endermann, R. Gahlmann, J. Krüger, S. Raddatz, Bioorg. Med. Chem. Lett. **13**, 241 (2003)
5. H.A. Stefani, C.B. Oliveira, R.B. Almeida, C.M.P. Pereira, R.C. Braga, R. Cella, V.C. Borges, L. Savegnago, C.W. Nogueira, Eur. J. Med. Chem. **41**, 513 (2006)
6. N. Hosseini Nasab, H. Raza, R.S. Shim, M. Hassan, A. Kloczkowski, S.J. Kim, J. Mol. Struct. **1286**, 135638 (2023)
7. A. Kumar, R.A. Maurya, Tetrahedron Lett. **48**, 4569 (2007)
8. N. Mohammadian, B. Akhlaghinia, Res. Chem. Intermed. **43**, 3325 (2017)
9. G. Van Der Heijden, E. Ruijter, R.V.A. Orru, Synlett **24**, 666 (2013)
10. M.M. Anastas, P.T. Kirchhoff, Acc. Chem. Res. **35**, 686 (2002)
11. R.A. Sheldon, Green Chem. **9**, 1273 (2007)
12. P. Beigiazaraghbelagh, A. Poursattar Marjani, Res. Chem. Intermed. **50**, 485 (2024)
13. S. Bibak, A. Poursattar Marjani, Sci. Rep. **13**, 17894 (2023)
14. A. Poursattar Marjani, F. Asadzadeh, A. Danandeh Asl, Appl. Organomet. Chem. **37**, 1 (2023)
15. A. Cornelis, P. Laszlo, P. Pennetreau, Clay Miner. **18**, 437 (1983)
16. G. Nagendrappa, Appl. Clay Sci. **53**, 106 (2011)
17. S. Bikas, A. Poursattar Marjani, S. Bibak, H. Sarreshtehdar Aslaheh, Sci. Rep. **13**, 2564 (2023)
18. J.M. Adams, K. Martin, R.W. McCabe, J. Incl. Phenom. **5**, 663 (1987)
19. S.D. Salim, K.G. Akamanchi, Catal. Commun. **12**, 1153 (2011)
20. J. Lal, M. Sharma, S. Gupta, P. Parashar, P. Sahu, D.D. Agarwal, J. Mol. Catal. A Chem. **352**, 31 (2012)
21. B. Vijayakumar, G.R. Rao, J. Porous Mater. **19**, 491 (2012)
22. P. Gupta, S. Paul, J. Mol. Catal. A Chem. **352**, 75 (2012)
23. R. Tayebee, M.M. Amini, M. Ghadamgahi, M. Armaghan, J. Mol. Catal. A Chem. **366**, 266 (2013)
24. F. Tamaddon, S. Moradi, J. Mol. Catal. A Chem. **370**, 117 (2013)
25. A. Rajack, K. Yuvaraju, C. Praveen, Y.L.N. Murthy, J. Mol. Catal. A Chem. **370**, 197 (2013)
26. J. Safari, S. Gandomi-Ravandi, J. Mol. Catal. A Chem. **373**, 72 (2013)
27. G. Kour, M. Gupta, S. Paul, Rajnikant, V.K. Gupta, J. Mol. Catal. A Chem. **392**, 260 (2014)
28. K. Kouachi, G. Lafaye, S. Pronier, L. Bennini, S. Menad, J. Mol. Catal. A Chem. **395**, 210 (2014)
29. Y. Titova, O. Fedorova, G. Rusinov, A. Vigorov, V. Krasnov, A. Murashkevich, V. Charushin, Catal. Today **241**, 270 (2015)
30. A. Mobinikhaledi, N. Foroughifar, A. Khajeh-Amiri, React. Kinet. Mech. Catal. **117**, 59 (2016)
31. D. Elhamifar, D. Elhamifar, F. Shojaeipoor, J. Mol. Catal. A Chem. **426**, 198 (2017)
32. M. Sheykhan, A. Yahyazadeh, L. Ramezani, Mol. Catal. **435**, 166 (2017)
33. J. Safaei-Ghomi, M. Tavazo, G.H. Mahdavinia, Ultrason. Sonochem. **40**, 230 (2018)
34. E. Dezfoolinezhad, K. Ghodrati, R. Badri, SILICON **11**, 1593 (2019)
35. R. Esmaeili, L. Kafi-Ahmadi, S. Khademinia, J. Mol. Struct. **1216**, 128124 (2020)
36. F. Ramezani Gomari, S. Farahi, H. Arvinnezhad, Iran. J. Chem. Chem. Eng. **40**, 888 (2021)
37. B. Mohammadi, F.K. Behbahani, G.B. Marandi, B. Mirza, Russ. J. Org. Chem. **58**, 1319 (2022)
38. F. Mohamadpour, Sci. Rep. **13**, 13142 (2023)

39. F. Mohamadpour, Polycycl. Aromat. Compd. (2023)
40. M. Nikpassand, L.Z. Fekri, M. Gharib, O. Marvi, Lett. Org. Chem. **9**, 745 (2013)
41. M. Kancherla, V. Badathala, J. Porous Mater. **24**, 1187 (2017)
42. B. Vijayakumar, G.R. Rao, J. Porous Mater. **19**, 233 (2012)
43. V. Singh, R. Ratti, S. Kaur, J. Mol. Catal. A Chem. **334**, 13 (2011)
44. X.X. Zheng, Z.P. Fang, Z.J. Dai, J.M. Cai, L.J. Shen, Y.F. Zhang, C.T. Au, L.L. Jiang, Inorg. Chem. **59**, 4483 (2020)
45. S. Sadjadi, M.M. Heravi, M. Malmir, Res. Chem. Intermed. **43**, 6701 (2017)